Radio Frequency Identification (RFID) on Textiles

Thesis

Presented in Partial Fulfillment of the Requirements for the Degree Bachelor of Science in Electrical and Computer Engineering of The Ohio State University

By

Junzi Xiang

Undergraduate Program in Electrical Engineering

The Ohio State University

2019

Thesis Committee:

Prof. Asimina Kiourti, Ph.D., Advisor

Prof. Robert J. Burkholder, Ph.D.

Abstract

Radio Frequency Identification (RFID) provides a convenient and efficient way of identifying targets with unique advantages over barcodes and Near Field Communication (NFC). However, traditional RFID systems are composed of rigid components, such as copper antennas and coin cell batteries, which prohibit their use in wearable scenarios. By contrast, this thesis explores fully flexible RFID tags that are based on textiles. Numerous applications are envisioned, such as RFID-enabled fabrics that detect open wounds or smart bed-sheets that sense wetness. In particular, this thesis focuses on the design, fabrication, and testing of RFIDs that operate at Ultra-High Frequencies (UHF) and may work as passive or as Battery-Assisted Passive (BAP). Three flexible materials are contrasted: (a) copper tape, (b) metalized fabric, (c) embroidered e-textiles. Experimental results show that copper tape RFID tags achieve the longest reading distance (1.32 m or ~4.3 ft), followed by metalized fabrics (99.1 cm or ~3.3 ft) and embroidered e-textiles (58.4 cm or ~1.9 ft). Activation of the BAP mode is shown to further boost the reading distance by 48.6 cm (~1.6 ft). Flexible implementations of such batteries are also discussed in this Thesis.

Acknowledgments

The author would like to express a sincere gratitude to Prof. Asimina Kiourti not only for the access of the experimental equipment in her Wearable and Implantable Technologies (WIT) laboratory, but also her advice and assistance in conducting this research. Special thanks give to all the members in Prof. Asimina Kiourti's group for offering precious experience and thoughts in the research progress.

Table of Contents

Abstract ii

Acknowledgments iii

List of Tables vi

List of Figures vii

Chapter 1: Introduction 9

1.1. Introduction to Wireless Identification Technology 9

1.2. Applications of RFIDs 10

1.3. Goals of this Research 12

1.4. Thesis Organization 12

Chapter 2: RFID System Analysis 14

2.1. RFID Operating Principle 14

2.2. Operating Modes Depending on Battery Usage 15

2.3. RFID Standards and Classifications 15

Chapter 3: Off-the-Shelf RFIDs: Programming and Performance 17

3.1. Nordic ID Stix RFID reader 17

3.2. Confidex Survivor B™ RFID tag 20

3.3. Battery-Assisted Passive (BAP) Mode Activation 23

Chapter 4: Finite Element Simulations of RFID Antenna 25

4.1. Replica of Confidex Survivor B™ RFID tag antenna 26

4.2. Design of T-match antenna 27

Chapter 5: Fabric-Based RFID Tag Prototypes 32

5.1. Copper tape RFID tag 32

5.2. Metalized fabric RFID tag 38

5.3. Embroidered e-textile RFID tag 39

Chapter 6: Experimental Results 43

6.1. Measurement set-ups 43

6.2. Measurement results 45

Chapter 7: Conclusions and Future Research 50

7.1. Conclusions 50

7.2. Future Research 51

References 53

Appendix A: Acronyms and Abbreviations 55

List of Tables

Table 1. ISO standards for RFID technologies 16

Table 2. RFID tag classifications 16

Table 3. T-match antenna selected parameters 31

Table 4. Maximum reading distance from passive to BAP mode 46

Table 5. Maximum reading distance of passive tags 47

List of Figures

Figure 1. Operating principle of Passive or Battery-Assisted Passive (BAP) RFIDs 14

Figure 2. Nordic ID Stix UHF RFID reader [10]..... 18

Figure 3. Nordic ID Stix Demo software [10] 19

Figure 4. Nordic reader inventory test [10] 19

Figure 5. (a) Confidex Survivor B™ RFID tag [11], (b) Radiation pattern [11]..... 20

Figure 6. (a) Survivor tag internal structure, (b) EM4325 chip board 21

Figure 7. Input impedance of Survivor antenna..... 22

Figure 8. Measured Survivor dielectric substrate 22

Figure 9. Characteristic impedance of EM4325 TSSOP8 [13]..... 23

Figure 10. BAP mode activation through Nordic Demo [10]..... 24

Figure 11. EM4325 TSSOP8 pins description [13] 26

Figure 12. Replica of Survivor tag (a) Top view, (b) Bottom view..... 27

Figure 13. T-match configuration and the equivalent circuit [15]..... 28

Figure 14. The matching chart for T-match for the case of $l = \lambda/2$, $w = \lambda/100$, $w' = 3/w$, $ZA = 75\ \Omega$ [15]..... 29

Figure 15. T-match antenna in HFSS 30

Figure 16. Copper tape T-match prototype test 33

Figure 17. Input impedance for copper tape T-match antenna from (a) HFSS simulation, (b) VNA..... 35

Figure 18. Copper tape T-match passive RFID tag prototype 1 36

Figure 19. Copper tape T-match BAP RFID tag prototype 1 (a) Top view (b) Bottom view 37

Figure 20. Metalized copper fabric passive RFID tag 39

Figure 21. E-textile passive RFID tag (a) 6 mm gap, (b) 4 mm gap 40

Figure 22. E-textile T-match prototype test with 4 mm gap 42

Figure 23. Directivity test schematic 43

Figure 24. Copper tape tag testing setup attached to the (a) top, (b) lateral side; (c) RFID reader set-ups 45

Figure 25. RSSI and Found percentage vs. distance for (a) Survivor tag, (b) Copper tape tag prototype 1, (c) Copper tape tag prototype 2, (d) Metalized fabric tag, (e) E-textile tag 49

Chapter 1: Introduction

1.1. Introduction to Wireless Identification Technology

A number of technologies have been reported to date for identification of objects, humans, and animals [1]. Some of the most well-known technologies entail barcodes, Radio Frequency Identification (RFID), and Near Field Communication (NFC).

Barcode is an optical representation of the data. It is composed of parallel lines with various widths and spacings, which can further be scanned by a remote device to read the represented information. However, barcodes are associated with several disadvantages, including: a) requirement for line-of-sight from the scanning emitter, b) limits of reading only one bar code at a time, c) degraded readability when barcodes get damaged or dirty, d) requirement for manual tracking, and e) inability to update the barcodes.

NFC is a wireless identification technology that works at the High Frequency (HF) of 13.56 MHz. Its operating principle relies on electromagnetic induction between two loop antennas. When the two antenna-bearing devices are placed close to each other, data can be automatically transferred. An advantage of NFC is that the associated reader cost is quite low. For example, NFC readers are already integrated in several commercial cell phone devices. However, NFC requires both devices to be placed in close proximity (typically a few millimeters). In turn, this limits NFC to only a small pool of applications (e.g., mobile payments by tapping on a machine reader).

On the contrary, RFIDs overcome the disadvantages above. In brief, RFIDs work by transmitting and receiving electromagnetic (EM) wave in various frequency ranges,

such as Low Frequency (LF), High Frequency (HF) and Ultra-High Frequency (UHF), to exchange information. They can be read regardless of line-of-sight, offer the feasibility of reading multiple tags simultaneously, do not require personnel involvement (can be tracked automatically), and offer the possibility of being reprogrammed. Currently, RFID technologies can be applied in different scenarios ranging from tracking the cargo or the labor environment in the supply chain management to body-worn electronics on humans.

1.2. Applications of RFIDs

RFID technology has been used for more than 60 years. In its early states, it was used in World War II by the allies and Germany to identify whether an aircraft was enemy or friend. Today, RFIDs are applied in numerous areas. In healthcare, tagging medicines using RFIDs can reduce medical errors. Vehicles at the toll station can make fast payment transactions (without stopping) through RFIDs that identify account holders. In library management, books can be self-checked out/in, and may automatically record the borrowing information eliminating manual labor. At store entrances/exits, RFIDs may be used to detect thefts. In this scenario, tags are attached to the items and can notify the shopkeeper if they pass through the gate sensor without permission [2].

More recently, RFIDs are becoming increasingly attractive in the textile industry. An Italian textile manufacturer, Griva, has deployed an RFID system for tracking the process of fabric production. In this example, barcodes cannot be employed as they become illegible under high temperature and extreme conditions associated with

industrial environments [3], [4]. Several other textile applications are envisioned for RFIDs, but have yet to take off because of limitations in the fabrication process.

As would be expected, RFIDs on textiles are better off to be lightweight, flexible, and inexpensive. Many state-of-the-art RFIDs claim to be based on textiles but are not robust enough to withstand bending or mechanical pressure. For example, RFIDs that rely on copper tape or conductive inks will readily crack and become inoperable within a few rounds of flexing or washing. By contrast, conductive e-threads are able to overcome such limitations and achieve the desired performance for textile applications. In this research, we take a step forward to explore RFIDs fabricated on e-threads, and identify opportunities for fully-flexible implementations that may eventually integrate fabric-based batteries as well. With the implementation of textile RFID systems, and taking into account the influence of the human body upon their performance, wearable devices can be applied into broader use, such as incontinence sensors on diapers or bedsheets, open wound detection and so on [5].

It is worth noting that robust textile-based RFIDs are not just limited to wearable applications. For some other elastic product manufacturing industries, such as tire companies, the advantages of RFIDs on textiles are increasingly superior to those achieved by typical rigid RFIDs. For example, tracking tires for stock management purposes may save labor cost. As another example, RFID tags can be attached to the tire itself as a way of monitoring its identity and other performance metrics while on use. Traditional RFID tags attached to tires rely on copper antennas that are vulnerable to shape distortion due to frequent transportation. This leads to degraded performance. By

contrast, textile-based RFID tags attached to the tire are preferred, as they are less affected by stretching and other deformations [6].

1.3. Goals of this Research

The goals of this research are:

1. Perform background research on RFID systems, and identify applications that may benefit from flexible, fabric-based RFID tags.
2. Identify materials that can be used to realize fabric-based RFID tags; explore fabrication methods to realize RFID antennas based on these materials; discuss merits/limits of each.
3. Build an RFID system that relies on the aforementioned fabric-based antennas; contrast the system's reading range performance for each scenario.
4. Explore the potential of realizing fully-flexible Battery-Assisted Passive (BAP) RFID tags on fabrics (i.e., realizing both the antenna and battery on fabrics).

1.4. Thesis Organization

This thesis is divided into seven chapters.

- Chapter 2 introduces the operating principle of RFID systems, including the theory and classifications of the RFID reader and tag, how they interact with each other, what kind of regulations they obey and the comparison of the performance and internal physical components among different RFID systems.

- Chapter 3 dives into the design and programming of a particular off-the-shelf UHF RFID system that is also capable of operating in either batteryless or Battery-Assisted Passive (BAP) mode.
- Chapter 4 illustrates the physical components of an RFID tag, mainly focusing on the antenna design.
- Chapter 5 discusses fabrication aspects of RFID antennas, focusing on materials, and particularly on fabric-based implementations.
- Chapter 6 describes the experimental setup and performance of various fabric-based RFID antennas.
- Chapter 7 provides a conclusion and suggestions for future research work.

Chapter 2: RFID System Analysis

2.1. RFID Operating Principle

RFIDs can be classified in terms of their operating frequency as Low Frequency (LF), High Frequency (HF) and Ultra-High Frequency (UHF). This thesis will focus on UHF (902-928 MHz) RFID systems. Such UHF RFID systems are composed of the RFID reader and the RFID tag. The RFID reader includes a transmitting antenna and various electronics for transmission and reception. The tag includes: a) an antenna for receiving and transmitting electromagnetic (EM) waves, b) an Integrated Circuit (IC) chip (e.g., EM4325) for storing the relevant information, and c) optionally a battery that may be activated for increased the reading range, per application requirements [7].

The RFID operating principle is demonstrated in Fig. 1. In principle, the RFID reader works as an interrogator sending out RF signals through a transmitting antenna to its surroundings. The tag, also known as the transponder, receives the signal and activates an internal chip to backscatter the RF signal with the stored information back to the reader. In doing, so, the tag is identified.

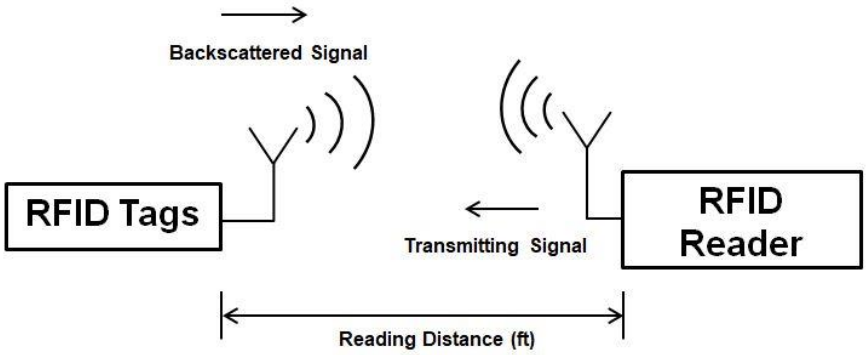

Figure 1. Operating principle of Passive or Battery-Assisted Passive (BAP) RFIDs

2.2. Operating Modes Depending on Battery Usage

Based on various operating modes of the UHF RFID tag (Passive, Active, Battery-Assisted Passive), the reading distance from the reader to the tag may significantly vary.

- Passive tags only consist of the antenna and an IC chip, which passively gets identified by the reader. These tags have a short reading distance up to 50 m (or about 164 ft).
- Active tags have extra on-board power supplies that enable much longer reading distances from the reader to the tag, enabling a longer reading distance from 30 cm (1 ft) to over 2 km (1.24 miles) [8]. The reason is that active RFID tags actively send out RF signals to the surroundings, regardless of the existence of the reader. In turn, these signals are captured and identified by the reader.
- Battery-Assisted Passive (BAP) tags also have built-in power supplies and the reading distance is in between the passive and active mode. Specifically, their operating mode is passive by default and can be modified by programming to BAP mode which offers increased reading distance. When the BAP mode is activated, the power supply will turn on and power the IC chip, increasing the reading distance for the backscattered signal to be captured by the reader.

2.3. RFID Standards and Classifications

Due to a variety of RF products in the market, it is significant to regulate the products and ensure their quality and safety. Regulations for RFIDs are mostly set by international organizations e.g., International Organization for Standardization (ISO) and industrial

organizations (e.g., GS1-EPCglobal) [9]. Based on the frequency the reader and tag operate on, ISO has set the international air interface standard shown in Table 1. According to the function of the RFID tag, various classes of EPCglobal are further assigned, as shown in Table 2. Here, read-only memory implies that the RFID tag can only be read and not be written by the RFID reader.

Table 1. ISO standards for RFID technologies

Standard Code	Air interface frequency
ISO 18000-V1	Reference Architecture and Parameters' Definition
ISO 18000-V2	135 KHz
ISO 18000-V3	13.56 MHz
ISO 18000-V4	2.45 GHz
ISO 18000-V5	5.8 GHz
ISO 18000-V6 (Type A, B, C, D)	860 MHz – 960 MHz
ISO 18000-V7	433.92 MHz

Table 2. RFID tag classifications

EPCglobal Tag Classes	Type of Tags	Functionality
Class 0	Passive	Read Only Memory
Class 1	Passive	Read Only Memory
Class 2	Passive	Read & Write Memory
Class 3	BAP	Read & Write Memory
Class 4	Active	Active Communication
Class 5	Active	Allow Communication with Class 4 & 5 tags

Chapter 3: Off-the-Shelf RFIDs: Programming and Performance

For the systematic understanding of RFID technology, off-the-shelf RFID systems are chosen to be explored first. Particularly, the Nordic ID Stix RFID reader [10] and Confidex Survivor B™ RFID tags [11] are selected in this research, because: (a) the Stix reader and Survivor tag are compatible in regulations and standards, (b) the Nordic reader with USB connectivity provides an interface software, Nordic Demo, that easily helps monitor the tag detections [10], (c) the Confidex tag enables activation of BAP mode which will further enhance our understanding of RFID operation, and (d) both the reader and tag are low-cost devices that can be readily acquired for research purposes.

It is worth noting that Survivor tags work in passive mode by default. They can be modified to BAP mode by toggling a bit in the designated location of the user memory bank in the IC chip. Such modification can be accomplished through the software interface of the reader. As stated in Chapter 2, the RFID reader sends out a signal with self-programmable power to the surroundings. The tag receiving the signal activates the internal IC chip and backscatters the signal to the reader with the stored information.

3.1. Nordic ID Stix RFID reader

Nordic ID Stix is an RFID reader (Fig. 2) with USB connectivity operating at UHF (902-928 MHz) and is regulated by the ISO 18000-63 (EPC Class 1 Gen2 V2) standard [10]. According to the regulations stating that an individual RFID reader cannot transmit the signal on the same frequency for more than 0.4 sec to avoid crowding frequencies (occupying one frequency for longer than 0.4 sec will create interference between

neighboring radio sources), the reader will “hop” every 0.4 sec across the frequency band in a preset pattern [12].

Figure 2. Nordic ID Stix UHF RFID reader [10]

The user interface software (Fig. 3) provided by Nordic can be installed on a laptop computer to: (a) self-program the RFID reader (e.g., power being sent out from the reader, modulation methods etc.), and (b) modify the tag operating type between passive and BAP mode. The latter will be discussed in Chapter 3.3. Fig. 4 shows an example of reading five Survivor tags simultaneously. Here, “Read Range” indicates the output power from the reader to its surroundings. This affects the reading distance in a way that the larger the output power, the further the reading distance between the reader and the tag. “Inventory Rounds” represents the number of rounds sending out power by the reader. “Continuous read” reads the tag in a preset speed while “single read” reads the tags only once [10].

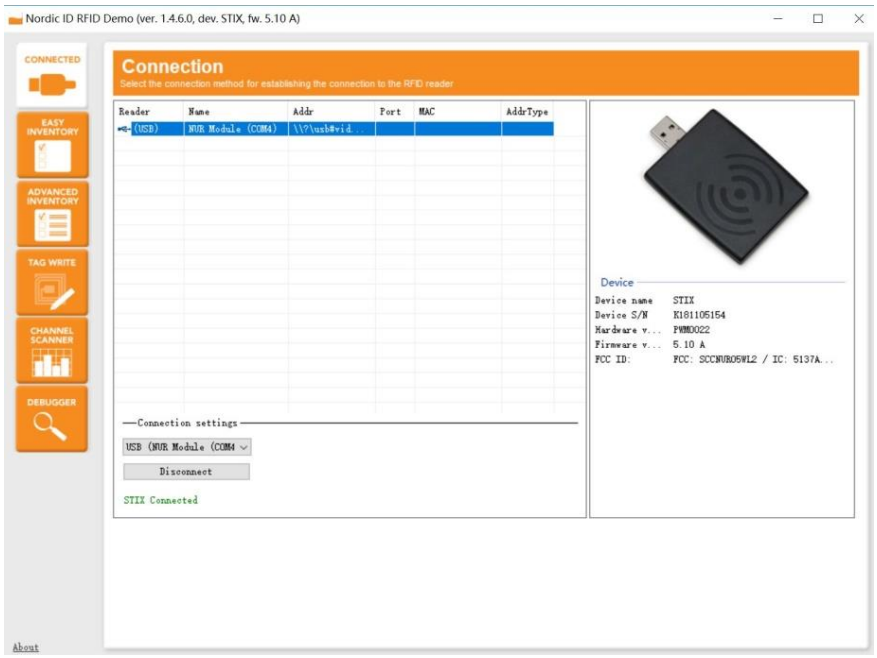

Figure 3. Nordic ID Stix Demo software [10]

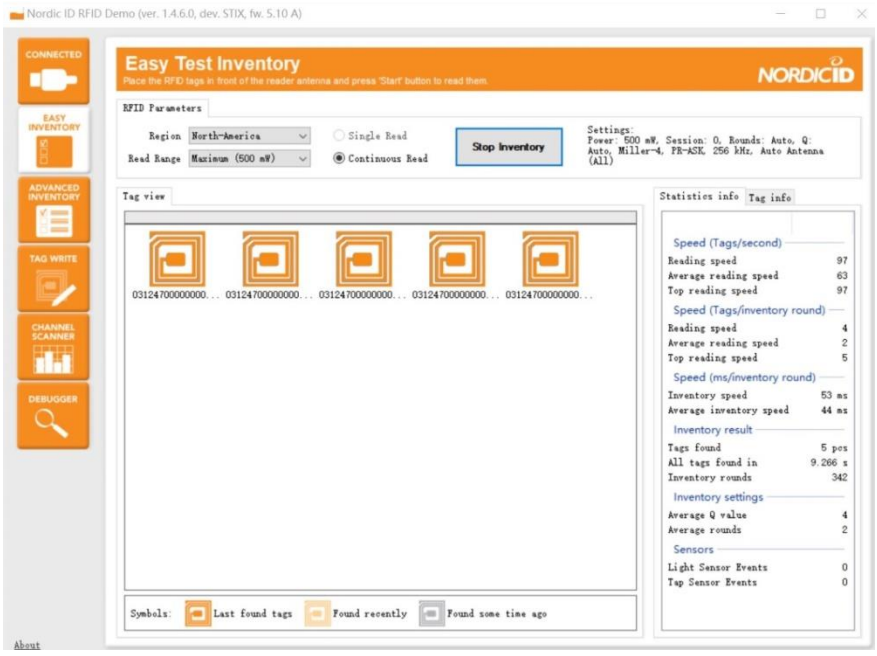

Figure 4. Nordic reader inventory test [10]

3.2. Confidex Survivor B™ RFID tag

The Confidex Survivor B™ RFID tag (Fig. 5) is compatible with the Stix reader and again operates in the UHF RFID band (902 - 928 MHz). It has a relatively small size (see Fig. 5a) and can be attached onto either dielectric materials or metals. Expectedly, radiation patterns and overall RFID performance will change in each case, as shown in Fig. 5b.

(a)

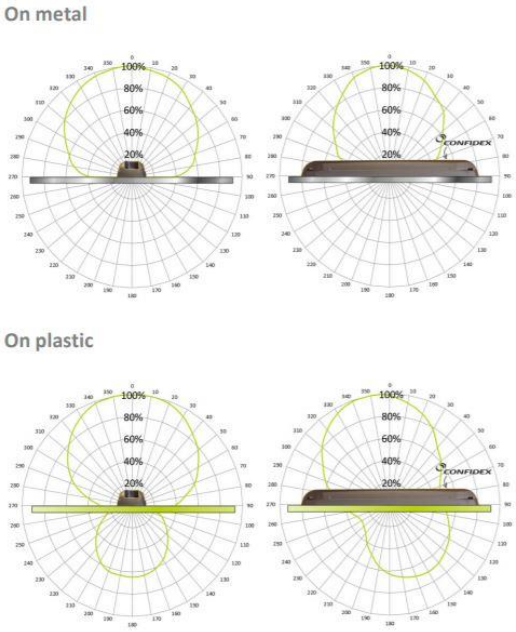

(b)

Figure 5. (a) Confidex Survivor B™ RFID tag [11], (b) Radiation pattern [11]

The internal structure of this tag is shown in Fig. 6. It has an internal coin cell battery that supports BAP mode activation. The internal antenna resembles a patch antenna and includes a copper strip and a ground plane. The antenna impedance is measured through a PNA-L N5235A Vector network analyzer (VNA) (see Fig. 7), and it is found to be equal to 15.99 + j148.2 Ω at 915 MHz. The antenna's dielectric material is measured using Keysight E4991A Impedance/Material Analyzer (Fig. 8) and it is found to have a relative permittivity ϵ_r close to 1 and a loss tangent of 0.0046 at 915 MHz. Theoretically, ϵ_r close to 1 provides convenience and possibility for converting the antenna into a fabric-based version, since ϵ_r for fabric substrate is typically close to 1. Besides, the tag utilizes the EM4325 IC chip that operates in passive mode by default and in BAP mode when activated through the user-defined programmable software. This can be realized through the Stix reader software. Fig. 9 shows the characteristic impedance of the EM4325 TSSOP8 package IC chip. Fig. 7 and 9 indicate that impedance of the Survivor antenna is almost conjugate matched with the chip's characteristic impedance at 915 MHz, which is critical for efficient power transmission between the antenna and the chip.

(a) (b)

Figure 6. (a) Survivor tag internal structure, (b) EM4325 chip board

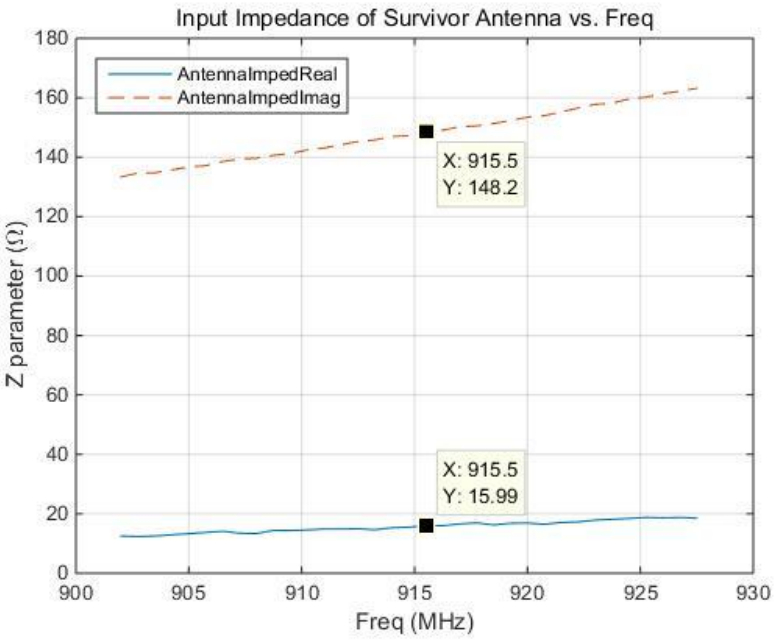

Figure 7. Input impedance of Survivor antenna

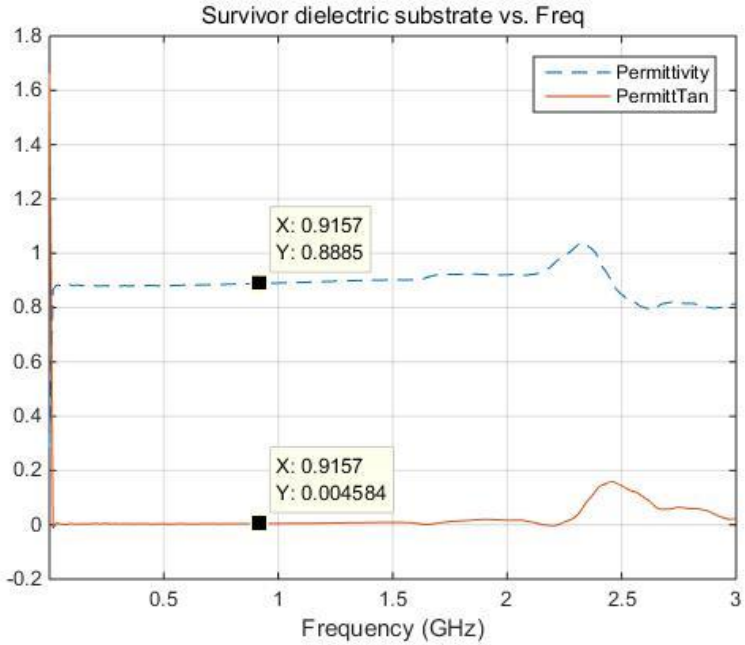

Figure 8. Measured Survivor dielectric substrate

Input impedance (between ANT+ and VSS) to be used for antenna matching optimized for passive mode	Z_{A_PAS}	BAP Mode disabled; P_{DUT} = -9dBm; Die form f_A = 866MHz f_A = 915MHz f_A = 953MHz		 18.1 - j169 15.2 - j159 14.9 - j154		 Ω Ω Ω
		BAP Mode disabled; P_{DUT} = -7dBm; TSSOP8 f_A = 866MHz f_A = 915MHz f_A = 953MHz		 23.3 - j145 17.6 - j113 14.5 - j95		 Ω Ω Ω

Figure 9. Characteristic impedance of EM4325 TSSOP8 [13]

3.3. Battery-Assisted Passive (BAP) Mode Activation

The Survivor tag works in passive mode by default. BAP mode can be either activated or de-activated by writing data into the "USER memory" bank of the EM4325 through Nordic Demo. Per the datasheet of Survivor tag [11] and EM4325 [13], toggling the last bit at system location 0x10D $(269)_{10}$ can turn on the BAP mode. However, it is word address mentioned in the document while the RFID Demo typically requires a byte address. And specifically, 1 word = 2 bytes in this case (1 word is not necessarily equal to 2 bytes in all cases). Word address 269 in decimal is byte address 538 in decimal (simply 2 times larger). In the Nordic Demo, one needs to choose "USER" in "TAG WRITE" and change the address in the memory to write data per Fig. 10. First, one has to read the memory from "Read Address" 538 bytes, then toggle the last bit, write 0, 0, 0, and 1 one by one and click on "Write to User memory" (it is better writing 0 to avoid undefined situation even if it already shows 0).

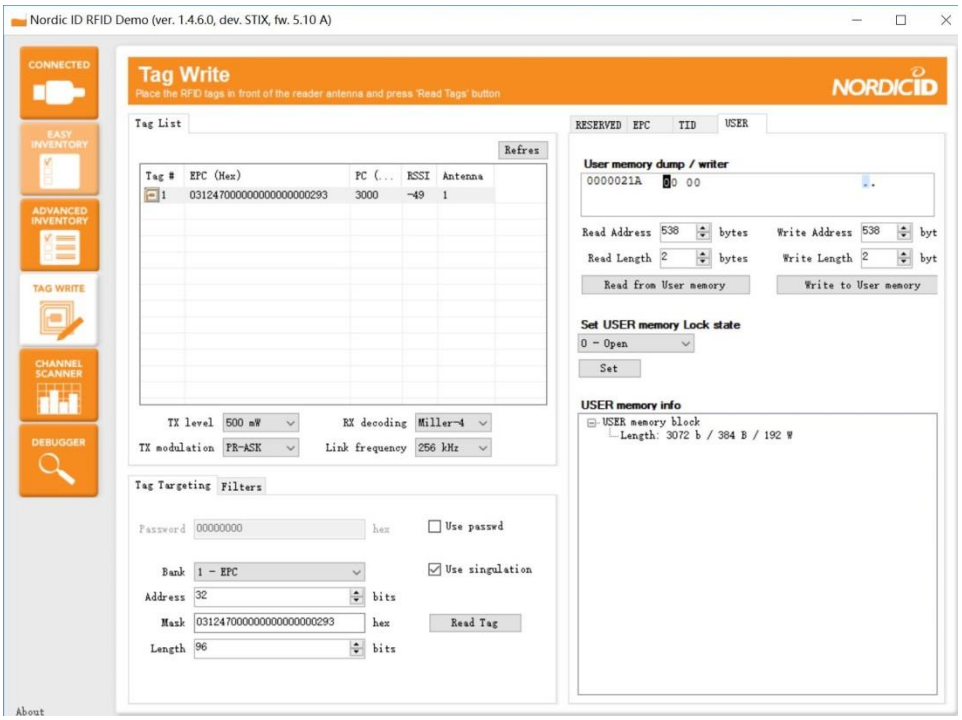

Figure 10. BAP mode activation through Nordic Demo [10]

The experiment showed that for passive mode of off-the-shelf Survivor tag, the maximum reading distance is 1.52 m (~5 ft). With BAP mode activation, the maximum reading distance is 2.18 m (~7.2 ft). Overall, transformation from passive to BAP mode leads to 66 cm (~2.2 ft) increase in reading distance, which matches with the expectation that RFID tags in BAP mode have increased reading distance as compared to passive mode.

Chapter 4: Finite Element Simulations of RFID Antenna

Generally, antenna implementation incorporates four steps – theoretical analysis, simulation analysis, fabrication, and measurement. In this thesis, a Finite Element software, ANSYS High Frequency Structure Simulator (HFSS), is used for simulation [14]. The ultimate goal is to simulate an antenna that is flat upon a fabric and matched to the EM4325 TSSOP8 package chip impedance at the UHF operating frequency range (902-928 MHz). Due to the variation of the chip impedance as a function of frequency, in this Thesis, we will only focus on the chip impedance of 17.6 - j113 Ω at 915 MHz [13]. Focusing on a single frequency throughout the implementation means at other frequencies, the antenna and the chip will not conjugate match perfectly, so that power loss is inevitable which will further cause degraded reading distance.

This chapter will be divided in two sections. First, an in-house replica of the Confidex Survivor antenna will be made to gain experience in simulations, fabrication, and measurements. This in-house tag can further be tested to confirm activation of the BAP mode. However, this is a 3D antenna (strip and ground plane separated by a substrate). As such, it is not suitable for 2D implementations on fabric. Thus, a new RFID antenna will be designed next, and particularly a T-match shaped antenna.

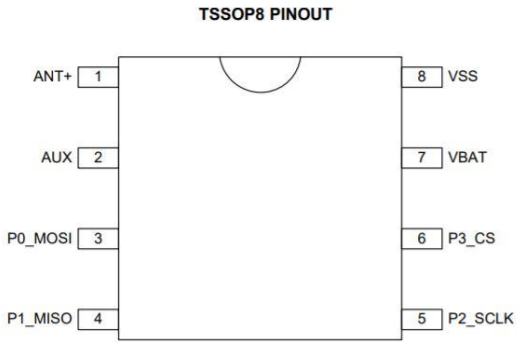

Pin	Name	I/O	Description
1	ANT+	A	Antenna +
2	AUX	I/O	Auxiliary Function
3	P0_MOSI	I/O	I/O P0 or SPI Master Output / Slave Input
4	P1_MISO	I/O	I/O P1 or SPI Master Input / Slave Output
5	P2_SCLK	I/O	I/O P2 or SPI Serial Clock
6	P3_CS	I/O	I/O P3 or SPI Chip Select (active low)
7	VBAT	A	External supply voltage for BAP operation
8	VSS	A	Supply return and Antenna -

A: Analog, I: Digital Input, O: Digital Output

Figure 11. EM4325 TSSOP8 pins description [13]

4.1. Replica of Confidex Survivor B™ RFID tag antenna

The replicated Survivor tag is shown in Fig. 12. The Printed Circuit Board (PCB) is removed and the original IC chip is replaced by an off-the-shelf EM4325 TSSOP8 chip. Fig. 12a shows the copper strip with an elongated tip connected to the EM4325 TSSOP8 pin 1 in the back. Fig. 12b shows the ground plane (copper tape) wrapping the back of the dielectric material measured in Fig. 8. The coin cell battery cathode (+) is connected to the EM4325 TSSOP8 pin 7 via a copper wire of diameter 0.254 mm and the anode (-) is soldered to the ground plane, per datasheet requirements [13]. In summary, the copper strip antenna is connected to EM4325 TSSOP8 pin 1, battery (+) to pin 7, battery (-) and copper tape ground to pin 8. To avoid short circuits, the EM4325 TSSOP8 is placed on

the dielectric substrate with the copper tape partially being stripped out so that other pins without connections behave as open circuits.

For this set-up, the maximum reading distance of the in-house BAP Survivor tag is 1.96 m (~6.4 ft), which is close to the maximum reading distance 2.18 m (~7.2 ft) obtained by the off-the-shelf Confidex Survivor tag in BAP mode. Some losses are introduced in this case due to diverse factors, such as soldering and the super glue that repositions the strip copper antenna to the dielectric substrate.

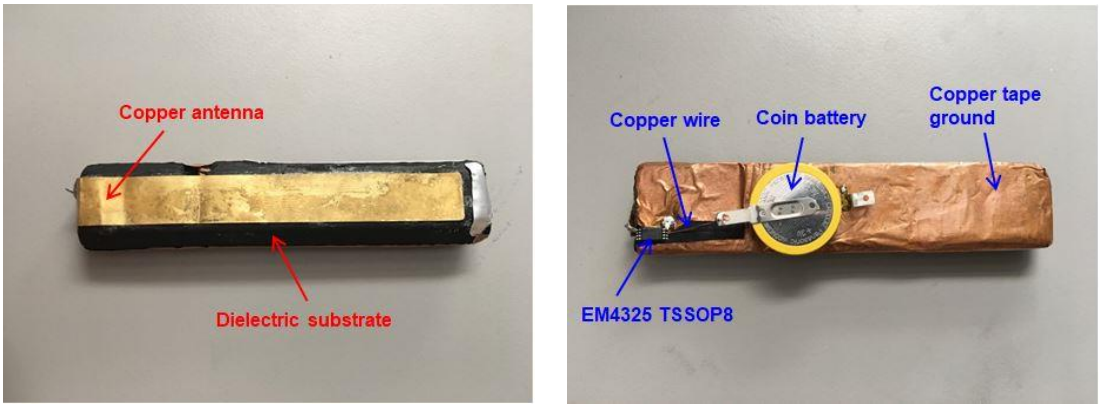

(a) Top view (b) Bottom view

Figure 12. Replica of Survivor tag (a) Top view, (b) Bottom view

4.2. Design of T-match antenna

The design of a particular type of RFID antenna starts with theoretical analysis. The T-match antenna (Fig. 13) is designed as a dipole antenna with a centered short-circuited stub. The feeding point to the T-match is at the second dipole with the length $a \leq l$, placed at horizontal distance *b* from the first dipole [15]. The input impedance is proven by [16], [17] to be

$$Z_{in} = \frac{2Z_t(1+\alpha)^2 Z_A}{2Z_t + (1+\alpha)^2 Z_A} \quad (1)$$

In short, the input impedance is the parallel combination of the half-wavelength dipole and the short-circuited stub dipole, where $Z_t = \mathrm{j}Z_0 \tan ka/2$ is the input impedance of the short-circuited stub, and for this particular dipole antenna, $Z_A = 73 + \mathrm{j}42.5\ \Omega$ [17].

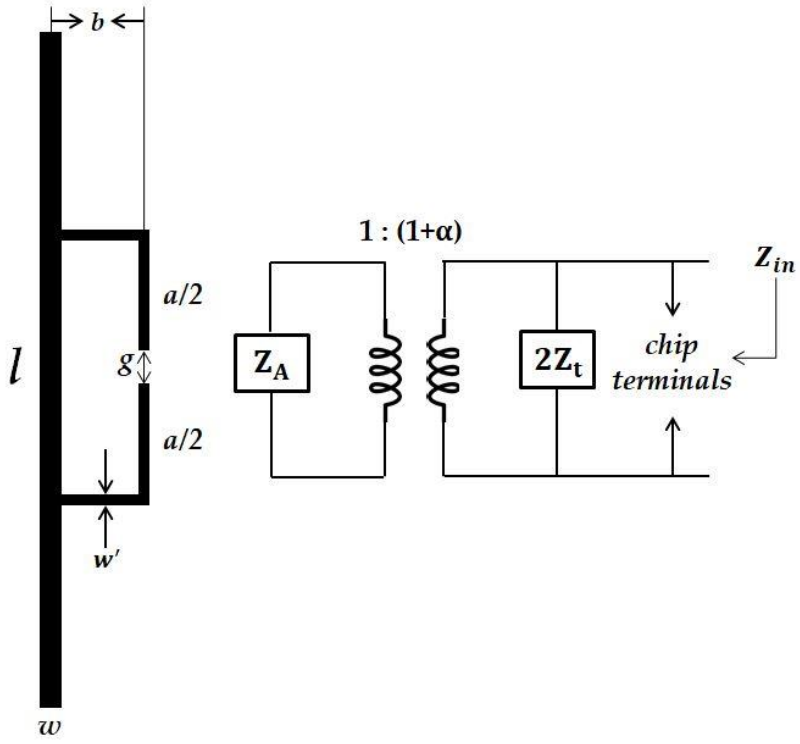

Figure 13. T-match configuration and the equivalent circuit [15]

The designed T-match antenna is intended to have its input impedance conjugate matched with respect to the chip, i.e. 17.6 + j113 Ω at 915 MHz. Referring to Fig. 13, *l* is chosen to be $\frac{\lambda}{2}$ where λ is the wavelength at 915 MHz via:

$$\lambda = \frac{c}{f} = \frac{3 \times 10^8 \text{ m/s}}{915 \times 10^6} = 327.9 \text{ mm} \quad (2)$$

Thus, $l = \frac{\lambda}{2} = 163.9$ mm. Referring to [15], $w = \frac{\lambda}{100} = 3.3$ mm, $w' = \frac{w}{3} = 1.1$ mm. Since the desired impedance is 17.6 + j113 Ω, *b/w* and *a/l* are estimated to be 1.5 and 0.1 respectively (Fig. 14). Therefore, *b* = 5.0 mm and *a* = 16.4 mm.

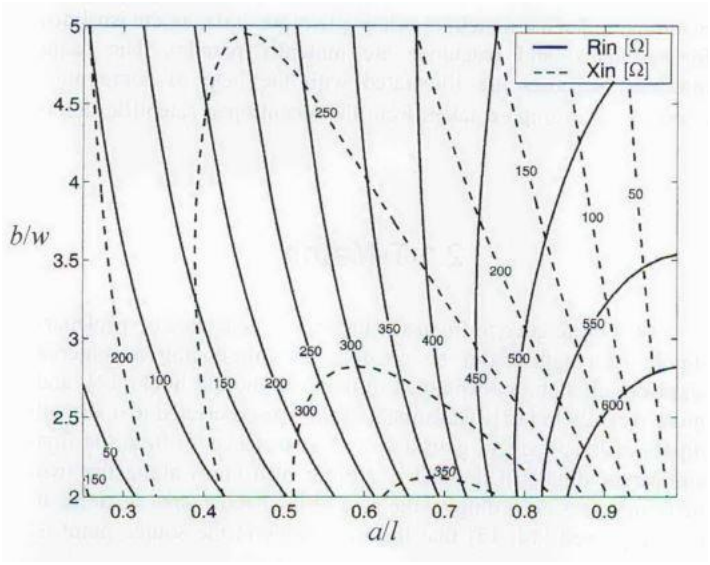

Figure 14. The matching chart for T-match for the case of $l = \lambda/2$, $w = \lambda/100$, $w' = 3/w$, $Z_A = 75\ \Omega$ [15]

As a next step, all aforementioned parameters are set as input to HFSS and the T-match antenna is designed, Fig. 15. The material for the antenna is selected as "Perfect E", which represents a perfect electric conductor (PEC). A radiation vacuum box is created

enclosing the antenna to test its far-field performance. The distance of the box is chosen at least $\lambda/4$ to each direction away from the farthest end point of the antenna. The parameter *g* which stands for the gap of the feeding port, is chosen to be 6 mm due to the pin-to-pin length of the EM4325 TSSOP8 being around 6 mm. In HFSS, a lumped port is chosen to feed the T-match antenna, whose typical characteristic impedance is 50 Ω. In practice, the feeding port will be the EM4325 TSSOP8 connected by soldering pin 1 and 8 to each terminal of the antenna (Fig. 11). In this case, the substrate of the T-match antenna is not taken into account because the ultimate goal is to fabricate the antenna through e-textiles whose substrate has a relative permittivity similar to air (i.e., $\epsilon_r = 1$).

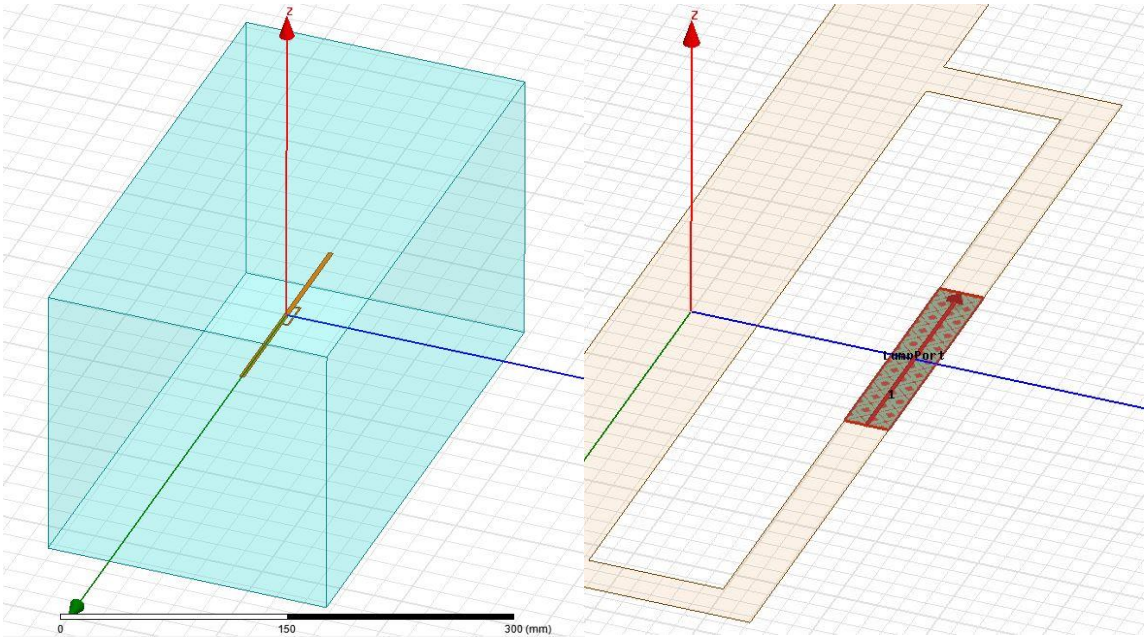

Figure 15. T-match antenna in HFSS

Through a parametric analysis that is performed to sweep the values of *a* and *b*, it is found that the optimal solution is an antenna impedance of 16.46 + j119.08 Ω that is

achieved at 915 MHz when a = 16.4 mm and b = 5.5 mm. The parameters for the T-match antenna are summarized in Table 3.

Table 3. T-match antenna selected parameters

Parameters	Length (mm)
l	163.9
w	3.3
w′	1.1
a	16.4
b	5.5
g	6

Chapter 5: Fabric-Based RFID Tag Prototypes

Based on the HFSS simulations, in this chapter, T-match antennas are fabricated and further soldered to the EM4325 TSSOP8 chip. Three flexible materials are employed– copper tape, metalized fabric, and embroidered e-textiles. Each has different performance due to the material type, feasibility of fabrication, and presence of a substrate. Overall, the copper tape based antenna with EM4325 TSSOP8 is found to exhibit the best performance in terms of reading distance. It is noted, however, that this is the only antenna that has Kevlar substrate ($\epsilon_r = 2.6$ [18]), while the substrate of the other two antennas is treated as $\epsilon_r = 1$. Additionally, for the copper tape RFID tag, BAP mode activation is tested by connecting an external coin cell battery to the fabric tag.

5.1. Copper tape RFID tag

The T-match antenna is made by cutting the copper tape to the size illustrated in Table 3. It is then attached to the Kevlar substrate. In order to verify the performance of the prototype versus the simulation result, it is connected through the VNA with (SubMiniature version A) SMA connector soldered to the antenna as shown in Fig. 16. The probe is connected to one of the two terminals while the outer conductor is connected to the other side of the antenna terminal.

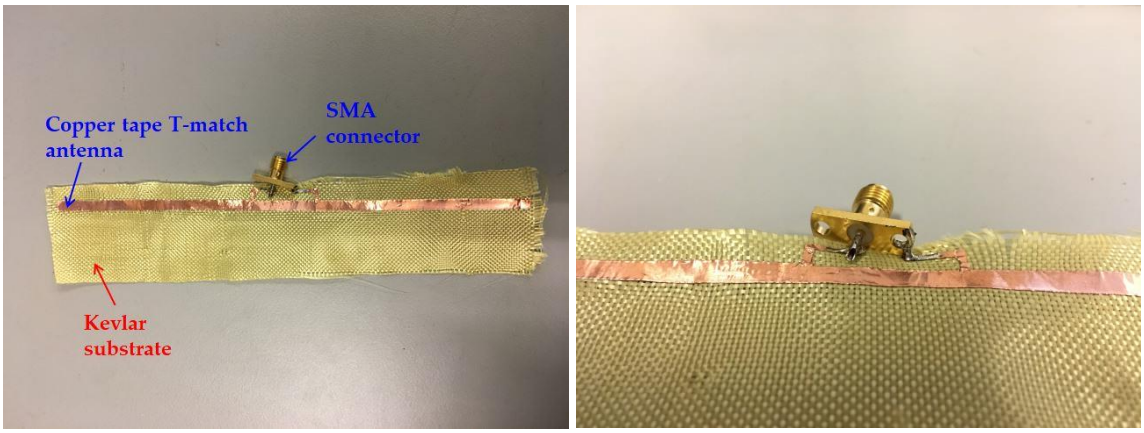

Figure 16. Copper tape T-match prototype test

Fig. 17 shows the result of input impedance from the HFSS simulation and VNA, respectively. At 915 MHz, HFSS simulation gives approximate 10 + j121 Ω while the VNA measurement of the prototype gives 175.1+j166.7 Ω. As seen, results show a large difference in the resistance, i.e., the real part of the impedance. The reason causing this might due to the fact that in the HFSS simulation, the conductor is PEC while in reality, the structure of copper tape would introduce some losses in terms of shape and material. The miniature size of the antenna makes it challenging to cut by hand and small deviation in dimensions will cause large error. Referring to Fig. 14, small variations in *b/w* and *a/l* contribute to significant errors in the input impedance. Soldering of the SMA connector also adds extra loss.

Accordingly, power reflection coefficient (in linear scale) can be calculated via:

$$|S11|^2 = \left|\frac{Z_c - Z_A^*}{Z_c + Z_A}\right|^2, \qquad |S11|^2 \in [0,1] \tag{3}$$

where Z_c stands for the characteristic impedance of the chip (17.6 – j113 Ω at 915 MHz) and Z_A represents input impedance of the antenna, Z_A is taken conjugate in the nominator to accommodate the fact that the both the chip and antenna impedance are complex number [19]. Power reflection coefficient describes the fraction of power that is reflected from the terminal, the larger the value, the less efficient the RFID tag will be. For convenience, power reflection coefficient typically is expressed in decibel (dB) scale via:

$$|S11|^2(\text{dB}) = 10\log_{10}\left|\frac{Z_c - Z_A^*}{Z_c + Z_A}\right|^2, \qquad |S11|^2(\text{dB}) \in [-\infty, 0] \tag{4}$$

Through calculation, $|S11|^2(\text{dB})$ for the actual copper tape tag at 915 MHz is -1.6 dB. Conventionally, an antenna design of having $|S11|^2(\text{dB}) < -10$ dB is of practical. Therefore, a relative large portion of power is not utilized by the chip from the antenna in the case of copper tape tag.

As noted above, the real part of the prototype's input impedance is not matched well to the EM4325 TSSOP8. In turn, reading range is expected to decrease as compared to the in-house Survivor RFID tag (Fig. 7). Details of reading distance results will be shown in Chapter 6.

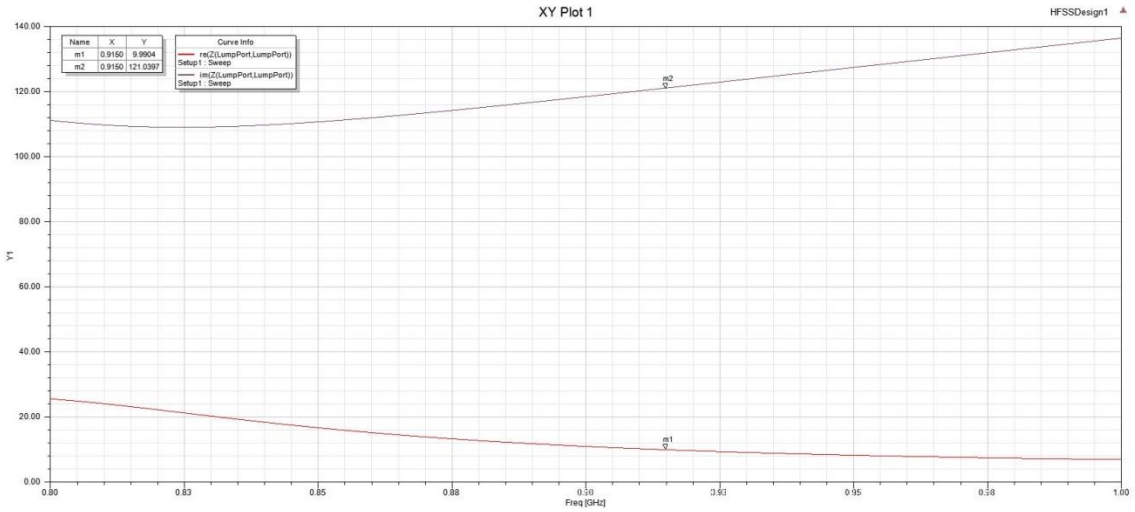

(a). HFSS simulation result

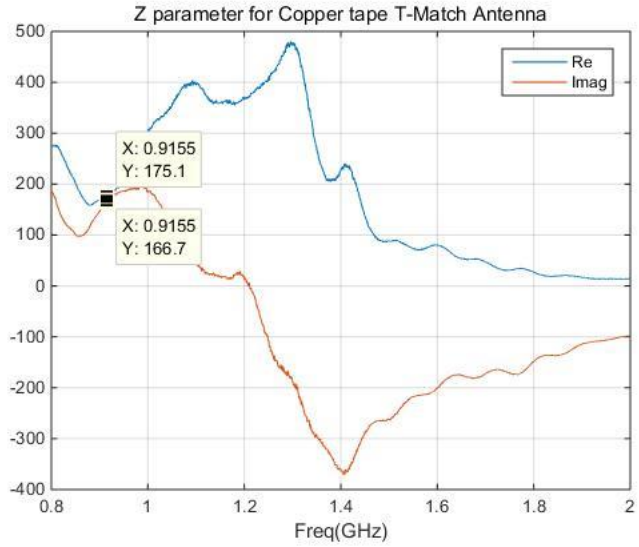

(b). VNA measurement

Figure 17. Input impedance for copper tape T-match antenna from (a) HFSS simulation, (b) VNA

After testing the antenna, the next step is to fabricate the passive RFID tag. To this end, the EM4325 TSSOP8 chip is soldered to the two terminals of the antenna with pin 1 on one side and pin 8 on other side, as shown in Fig. 18. Note that all pins, expect for pin 1 and 8, are connected as if they are open circuits since they are all attached directly to the dielectric Kevlar substrate. In short, the configuration acts as a passive RFID tag. Throughout the experiment, it can be detected by the Stix reader, having a maximum reading distance of 91.4 cm (~3 ft).

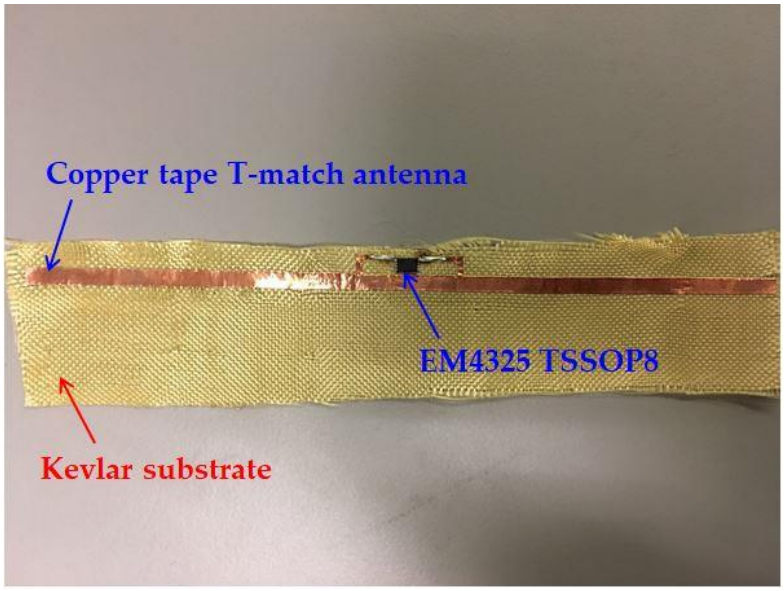

Figure 18. Copper tape T-match passive RFID tag prototype 1

Since the EM4325 TSSOP8 supports BAP mode, one further research step has been performed to explore its detection by the Stix reader with the BAP mode activated. In addition to the components in the passive tag, an extra coin cell battery (available voltage ~ 1.5 V) is connected to the EM4325 TSSOP8 as in Fig. 19. Per requirements in the datasheet (Fig. 11), the coin cell battery cathode (+) is connected to EM4325 TSSOP8

pin 7 and the anode (-) to pin 8. Although the result shows that the reading distance is boosted due to the battery activation, the behavior of the BAP tag is extremely unstable in a way that: a) the reading distance varies from time to time, b) in some circumstances the reading distance will be smaller than the tag without the battery operating in passive mode, and c) in certain cases two identities are detected even if only one tag is in the surroundings of the Stix reader. The reason causing two identities to be detected is possibly due to the characteristics of the EM4325 TSSOP8 configuration. A potential solution would be to modify the memory bank in particular locations, or replace the EM4325 with other packages.

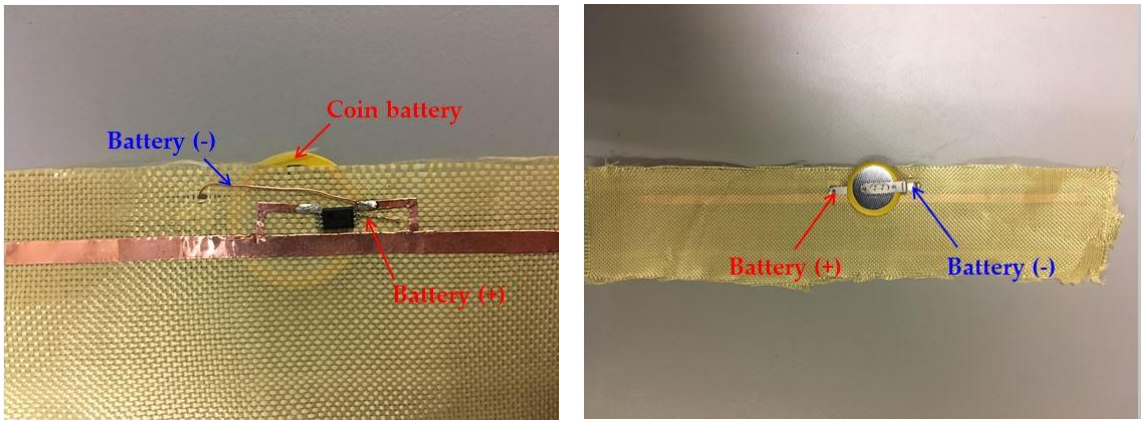

(a). Top view (b). Bottom view

Figure 19. Copper tape T-match BAP RFID tag prototype 1 (a) Top view (b) Bottom view

To assess repeatability, two identical copper tape prototypes are made and tested in passive mode. However, as mentioned before, even the same tag performs differently when the measurements are taken at different time. Two identical tags differ in their reading distance performance. The first prototype made for BAP mode activation has

maximum reading distance of around 91.4 cm (~3 ft) in passive mode. The second passive prototype reaches a maximum of 1.27 m (~4.2 ft) when it is placed on the top and 1.32 m (~4.3 ft) when it is attached to the lateral face of the Styrofoam. The inconsistency of two prototypes with the same dimensions needs to be improved and will be discussed in Chapter 7.

5.2. Metalized fabric RFID tag

As a transition from the copper tape to the e-textile RFID tag, metalized copper fabric is used in between. In this case, no dielectric substrate is employed and the tag is placed upon Styrofoam for testing (Fig. 20). Through experiments, the metalized fabric tag shows 33 cm (~1 ft) smaller maximum reading distance than the copper tape tag. The degraded performance is largely due to the fabrication since cutting the T-match arms in 1.1 mm is not easy enough. Also, the metalized fabric is not in a high density in the sense that the fabric is composed of copper strips grouped together so that gaps exist in the spacings, which makes the fabric less conductive than expected. Overall, the inferior performance can be compensated if more careful fabrication is done and denser metalized fabric is used.

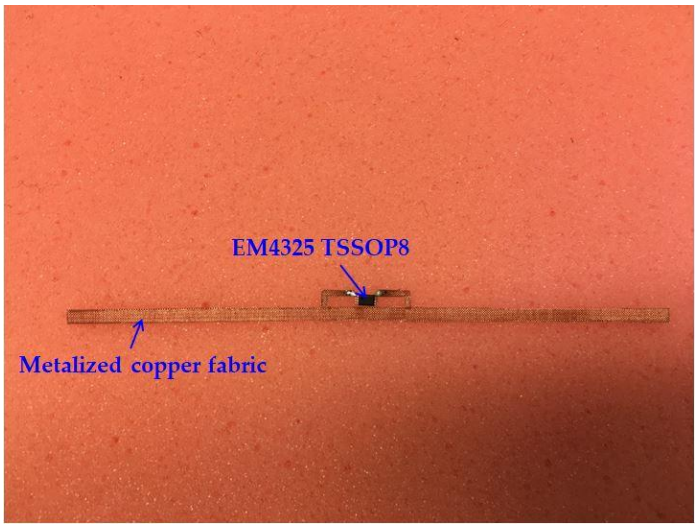

Figure 20. Metalized copper fabric passive RFID tag

5.3. Embroidered e-textile RFID tag

Beyond using copper tape and metalized fabric, lastly, the tag is fabricated by e-threads using an automated embroidery process (Fig. 21). The first prototype is realized as the original dimension designed from Table 3. Due to the difficulties in soldering (both Elektrisola-7 e-threads and the fabric substrate are vulnerable to high temperature, which will be burnt easily), the gap in between the two terminals of the antenna is adjusted to 4 mm. The other parameters stay the same so that two pins of the EM4325 chip align on the top of the terminals. The result shows that it makes no difference in the performance for the two tags because both achieve the same maximum reading distance of 58.4 cm (~1.9 ft).

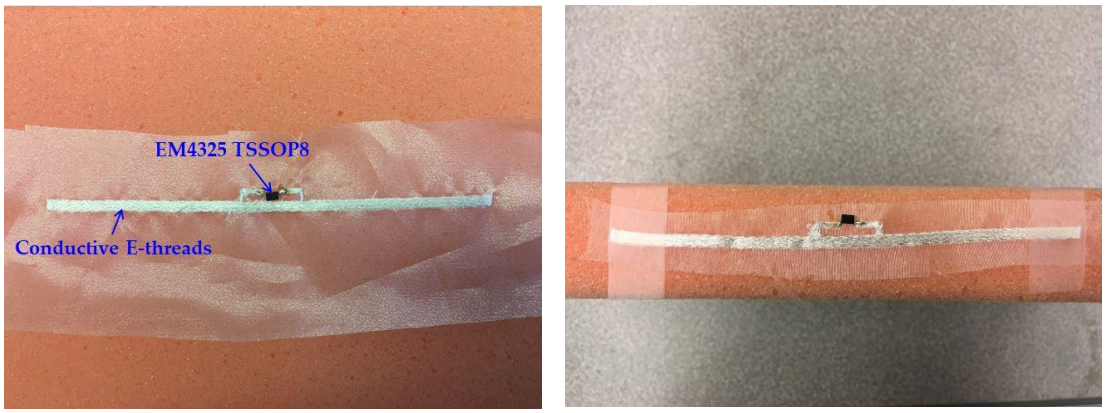

(a). Prototype 3 with 6 mm gap (b). Prototype 4 with 4 mm gap

Figure 21. E-textile passive RFID tag (a) 6 mm gap, (b) 4 mm gap

For prototype 3, the embroidery direction moves horizontally back and forth from left to right throughout the whole portion of the antenna. For prototype 4, the direction is a little different in the sense that the threads' direction of the T-shape arm between the two dipoles moves vertically. Practically speaking, the error for achieving the width $w' = 1.1$ mm across the arm and the smaller dipole is not negligible due to the miniature dimension. As such, e-threads across the arm move vertically to ensure that the width is equal to 1.1 mm. After all, there is no difference in the performance of the tag, with details shown in Chapter 6.

The e-textile antenna is tested through the VNA with SMA connection in between the ports (Fig. 22). The inner conductor of the SMA connector is connected to the left terminal and the outer conductor is connected to the right. The input impedance from the VNA gives an impedance of 307.7+j110.9 Ω. As seen, the resistance is much larger than that of the copper tape, which further decreases the performance of the tag. This is within

expectation due to the calculation $|S11|^2(\text{dB}) = -1$ dB, which is larger than the power reflection coefficient for the copper tape.

Through the prototype measurement, it is found out that the maximum reading distance decreases to 40.7 cm (1.3 ft) compared to the metalized fabric tag. On the other hand, in the HFSS simulation, no substrate ($\epsilon_r = 1$) is used and, referring to Chapter 4.2, Z = 16.46 + j119.08 Ω. The difference in the result between simulation and measurement lies in that for the fabrication, 7 e-threads/mm is used and the diameter of a single thread is 0.1 mm. Thus, during the embroidery process, for 1 mm length in the designed dimension, merely 0.7 mm of e-threads are the conductive part of the antenna. Combing with the fact that the conductor in HFSS simulation is PEC, more losses are inevitable to the actual implementation. Compared to the other two tags (copper and metalized fabric), e-textile RFID tags give the worst result mainly because of the complexity of e-thread embroidery. Specifically, the embroidery machine cannot achieve very fine details such as the widths and gaps in the design due to the imperfect metallization of the textile surface [20].

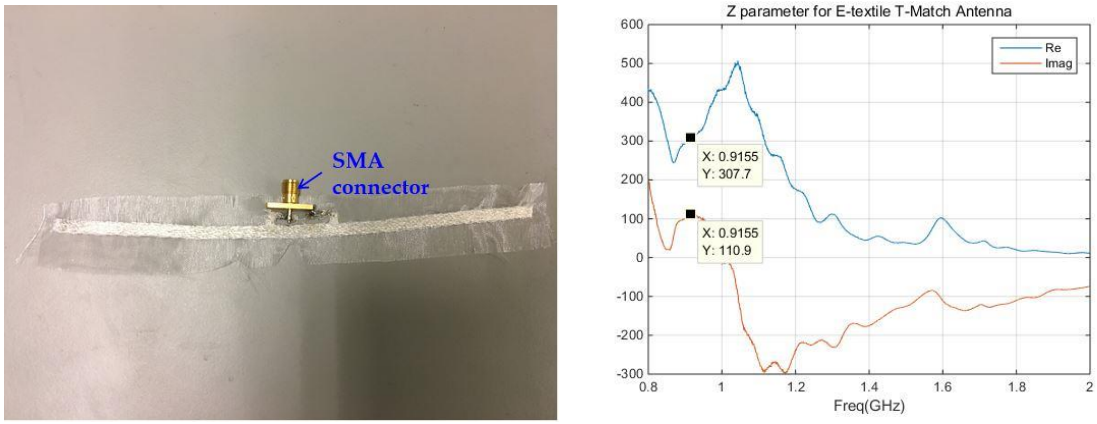

Figure 22. E-textile T-match prototype test with 4 mm gap

Chapter 6: Experimental Results

Measurements are taken mainly by attaching the tags either on the top or the side of the Styrofoam and moving in certain distances from the Stix reader. For the reference of the received power from the tag, the received signal strength indication (RSSI) is monitored and recorded using the Nordic Demo. In addition, the directivity of the tag is tested as indicated in Fig. 23 viewing from the top. The angles θ and φ are measured, which represent the detection angles between the tag (moving upside down) and the reader.

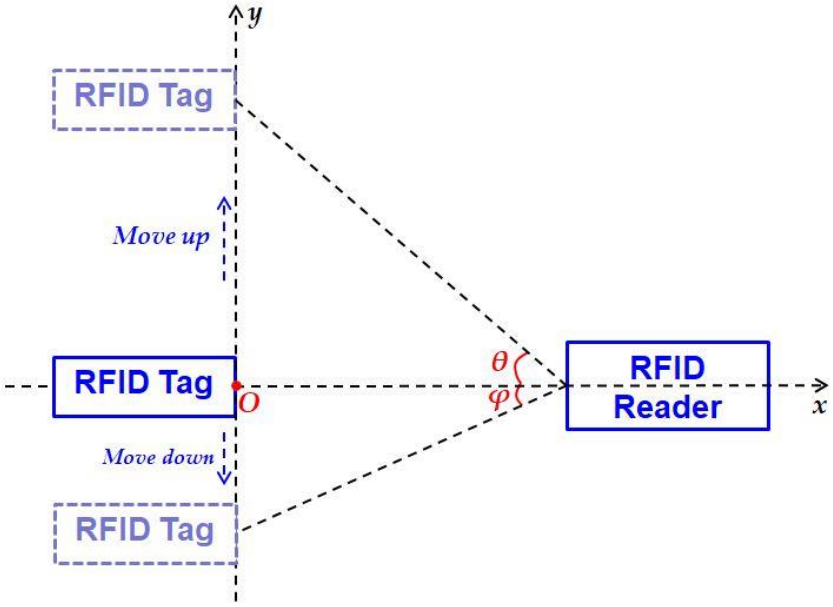

Figure 23. Directivity test schematic

6.1. Measurement set-ups

For the purpose of avoiding interference from the surroundings during the measurement (the dielectric property of the table would detune the antenna if the tag is placed on the table directly), the fabric-based RFID tag prototypes are attached to the top and lateral

face of a Styrofoam block ($\epsilon_r = 1$). Examples of the setups for the copper tape tag are shown in Fig. 24. The metalized fabric tag and e-textile tag are tested when they are attached to the side of the Styrofoam since the tags on the lateral face give better performance than being placed on the top. Directivity is tested by moving the tag with the table up and down viewing from the top with a fixed reading distance from the reader. The maximum reading distance is recorded when the tag is detected by the reader exactly at a certain position, further than which the reader is not able to detect the tag. The Nordic Stix RFID reader is set to a maximum RF power of 500 mW, which ensures that the reader is working at the maximum read range. However, it does not mean that the power consumption of the reader is 500 mW, in fact, it consumes 3 W [10]. Miller-4 and PR-ASK represent the receiver decoding and transmitter modulation of the reader, respectively. 256 KHz is the selectable link frequency between the reader and the tag communication out of the options among 160 KHz, 256 KHz and 320 KHz. Higher link frequency leads to higher data transmission speeds while is more susceptible to bit errors [10]. Measurements are carried out by reading the tags at approximately 100 inventory rounds and meanwhile, RSSI is recorded. Although the experimental results vary by time, the results shown in 6.2 are generalized and well represent the tendency of the tags' performances.

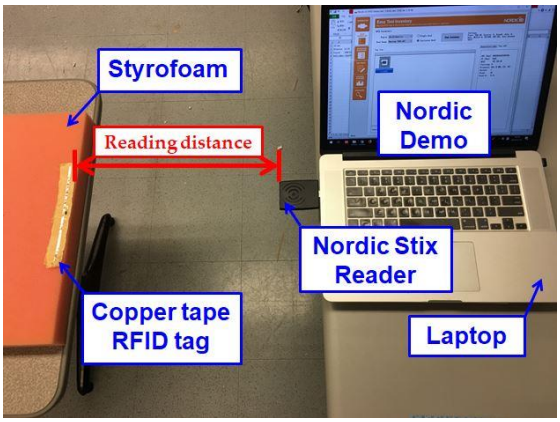

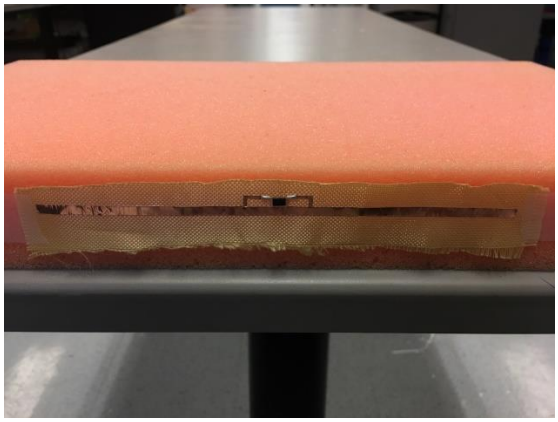

(a). Copper tape attached on the top (b). Attached to the lateral face

```
Settings:
Power: 500 mW, Session: 0, Rounds: Auto, Q:
Auto, Miller-4, PR-ASK, 256 kHz, Auto Antenna
(All)
```

(c). RFID reader setups

Figure 24. Copper tape tag testing setup attached to the (a) top, (b) lateral side; (c) RFID reader set-ups

6.2. Measurement results

The maximum reading distances of the tags are summarized in Table 4. Reading distance is measured in cm/m and approximated to the nearest feet with the step of 0.1 ft. It is therefore verified that BAP mode activation increases the reading distance by at least 48.6 cm (1.6 ft). However, once the fabricated tags utilize the EM4325 TSSOP8 and the coin cell battery, they automatically operated in BAP mode. The operating mode cannot be modified back to passive through the memory bank bit toggling described in Chapter 3.3 since the “USER memory” bank is locked and not writable. Consequently, detaching the battery connection to the chip will modify the fabricated BAP tag back to passive. For

comparison, two identical copper tape tags are made, one for BAP mode usage and the other is only used for passive mode operation.

Table 4. Maximum reading distance from passive to BAP mode

Maximum reading distance (cm/m or ft)	Confidex Survivor Passive 1.52 m (5 ft)	Confidex Survivor BAP 2.18 m (7.2 ft)	In-house Survivor BAP 1.96 m (6.4 ft)	Copper tape passive prototype 1 91.4 cm (3 ft)	Copper tape BAP prototype 1 1.4 m (4.6 ft)
RSSI (dBm)	-55	-74	-75	-64	-77
Found %	90	5	26	52	31

Apart from proving the increased performance when the operating mode changes from passive to BAP, Table 5 summarizes the maximum reading distance for all fabricated passive tags. It is observed that the performance degrades as the materials being used become more and more complicated and difficult to fabricate. Approximate 30.5 cm (~1 ft) decreased maximum reading distance is detected from the copper tape tag to the metalized fabric tag and to the e-textile tag. Fig. 25 shows the RSSI and found percentage with respect to the reading distance for each individual tag. In summary, copper tape is the easiest to fabricate since it is flexible and malleable so that one can realize it manually while the e-textile is the hardest to fabricate because of the complexity in stitching direction, the choice of the e-threads and the software simulation preparation. However, e-textile will be the candidate due to its robust performance. The performance of the copper tape and metalized fabric suffer from the cracking and flexing of materials and e-textile is proven having strong mechanical tolerance without affecting the performance [6].

Table 5. Maximum reading distance of passive tags

Maximum reading distance (cm/m or ft)	Copper tape passive prototype 2 placed on the top of Styrofoam 1.27 m (4.2 ft)	Copper tape passive prototype 2 attached to the side of Styrofoam 1.32 m (4.3 ft)	Metalized fabric passive 99.1 cm (3 ft)	E-textile 6mm gap 58.4 cm (1.9 ft)	E-textile 4mm gap 58.4 cm (1.9 ft)
RSSI (dBm)	-61	-62	-63	-60	-63
Found %	56	92	56	65	25

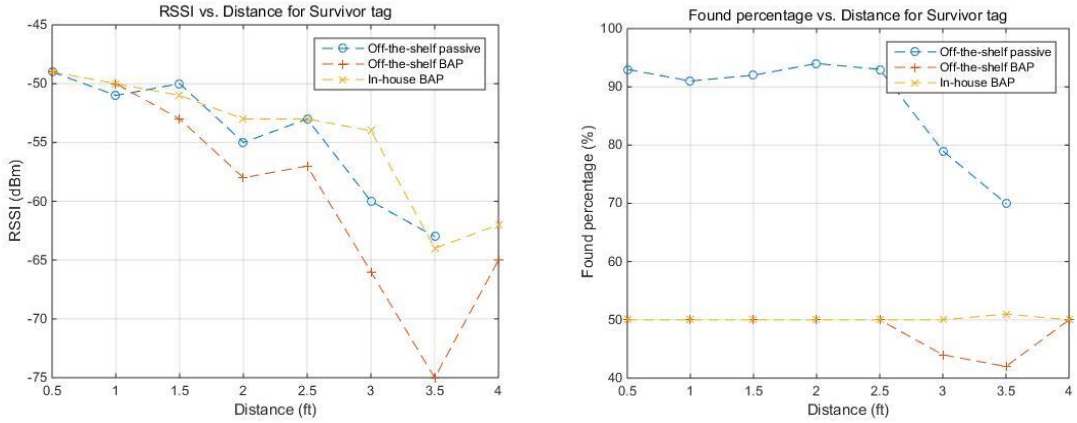

(a) Survivor tag RSSI and found percentage vs. distance

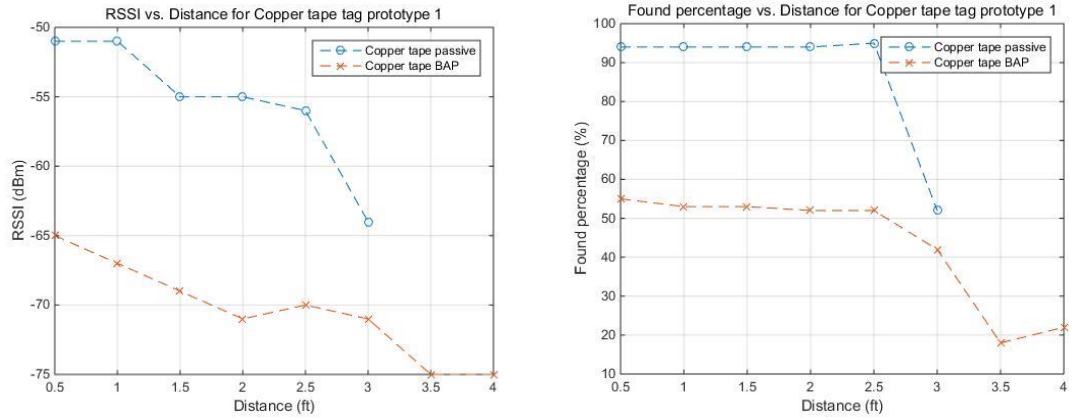

(b) Copper tape tag prototype 1 RSSI and found percentage vs. distance

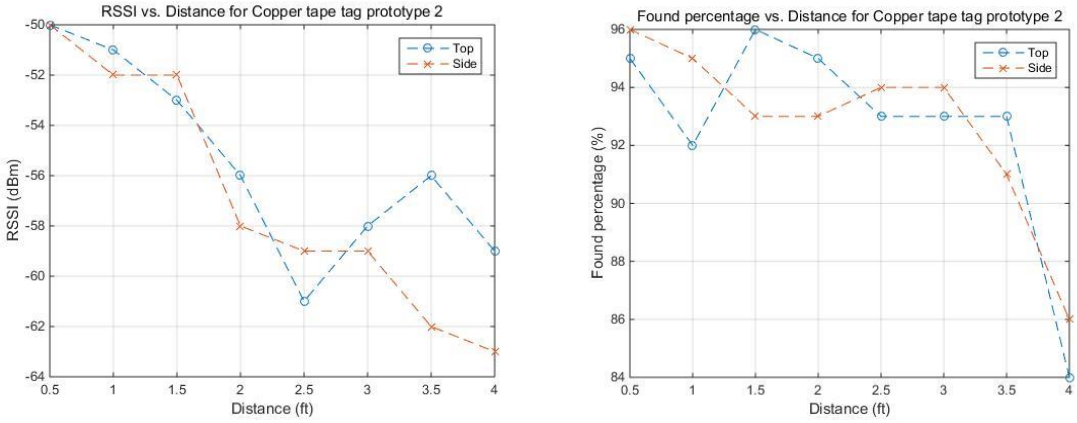

(c) Copper tape tag prototype 2 RSSI and found percentage vs. distance

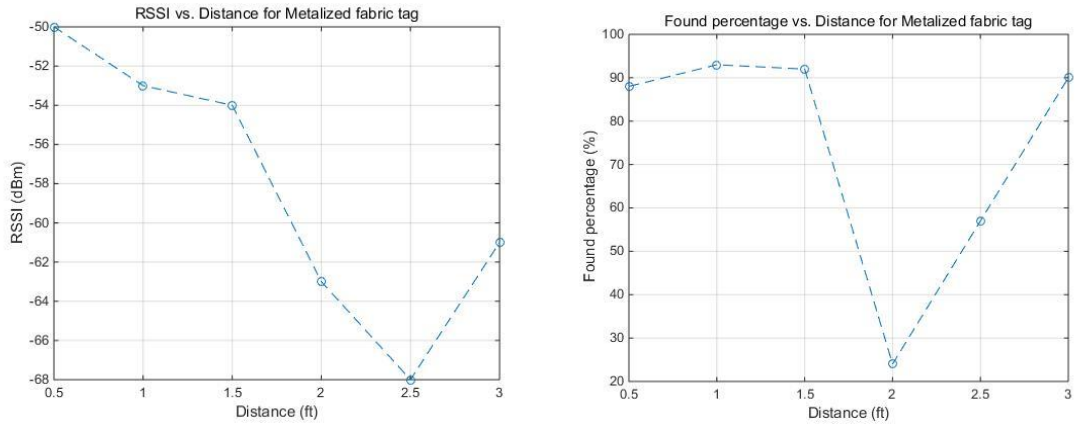

(d) Metalized fabric tag RSSI and found percentage vs. distance

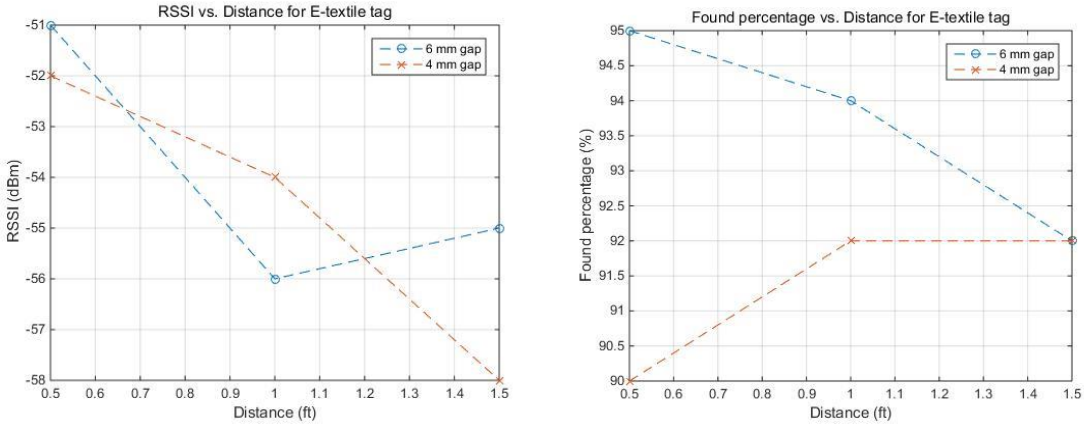

(e) E-textile tag RSSI and found percentage vs. distance

Figure 25. RSSI and Found percentage vs. distance for (a) Survivor tag, (b) Copper tape tag prototype 1, (c) Copper tape tag prototype 2, (d) Metalized fabric tag, (e) E-textile tag

Chapter 7: Conclusions and Future Research

7.1. Conclusions

This thesis starts with an overview of RFID systems as it relates to applications, operating principles and regulations. It then discusses materials used to fabricate fabric-based RFID tags, of which fabric-based antennas are designed and tested. Next, operating performances of RFID tags are compared between the passive mode and BAP mode activation for both a conventional off-the-shelf RFID tag and the in-house fabric-based tags.

Throughout the experiment, it is found that the off-the-shelf Survivor tag operates in passive mode by default and can be transformed into BAP mode by writing the data into a specific location in the IC chip. EM4325 TSSOP8 package IC chip particularly does not support transferring back from BAP mode to passive mode, as indicated in the in-house BAP Survivor tag and copper tape tag prototype 1. Further, activation of BAP mode boosts the performance of the RFID tag by at least 48.6 cm (1.6 ft). The performance of the passive textile RFID tags in terms of maximum reading distance ranks from high to low among the copper tape tag prototype 2, metalized copper tag and embroidered e-threads tag. Among the 3 prototypes, the copper tape and metalized copper tags are realized by cutting the materials using scissors. The e-thread tag is realized via an embroidery machine. Compared with the HFSS simulation result, it is concluded that the fabrication process degraded the tags' performance since the actual materials are not PEC, and dimensions of the T-match antenna are not exactly matched with the ones in the simulation due to manual errors in the fabrication process. Besides,

soldering the EM4325 TSSOP8 to the antenna terminal also creates a difference, more careful soldering skill is required.

7.2. Future Research

The first future work is to get a better agreement between simulation and measurement results for the antenna's part. This can be realized through more refined fabrication processes to match the actual fabricated sizes with the designed parameters. On the other hand, higher accuracy of the material can improve the results such as using denser metalized fabric and e-threads.

As another step, ongoing research on textile materials provides insights into fabricating a fully flexible BAP RFID tag, which combines embroidered e-textile antennas with fabric batteries. The envisioned fully-flexible integrated system will eliminate issues with existing technologies that require bulky batteries, low-efficiency harvesters, and/or rigid antennas. An example is an electrochemical fabric battery which, when moistened by a conductive bodily liquid (sweat, wound fluid, etc.), can generate DC voltage and current levels capable of powering wearable electronics on the go [21]. Generation of DC power is achieved via an electrochemical process that enables transfer of electrons from silver- to zinc-printed electrodes (anodes and cathodes), using the conductive liquid as an electrolyte. The minimum voltage required to power the tag in BAP mode, according to the datasheet of a typical IC chip, is 1.25V [13], which can be generated by two or more electrodes connected in series in this fabric battery. Besides, the maximum current required to power the chip is less than 10μA, which is also within

the current generation range of the fabric battery [21]. Therefore, conventional cumbersome battery of traditional BAP RFID tag can be replaced by innovative fabric-based electrochemical batteries. Example applications include smart garments for open-wound detection, smart bed-sheets for wetness sensing, and so on, where bodily conductive liquids such as wound fluid, sweat, or urine, may readily activate the battery. Contrary to conventional power generation techniques, the integrated BAP RFID tag is fully flexible, feels and behaves like regular clothing, and does not include any rigid components.

References

[1] G. R. White, G. Gardiner, G. Prabhakar, and A. A. Razak, “A Comparison of Barcoding and RFID Technologies in Practice,” *Journal of Information, Information Technology, and Organizations (Years 1-3)*, vol. 2, pp. 119–132, 2007.

[2] D. Parkash, T. Kundu, and P. Kaur, “The RFID Technology and its Applications: A Review,” International Journal of Electronics, Communication & Instrumentation Engineering Research and Development (IJECIERD), vol. 2, no. 3, pp. 109–120, Sep. 2012.

[3] M. Barburski, B. Czekalski, and M. Snycerski, “RFID Technology in the Textile Industry,” AUTEX Research Journal, vol. 8, no. 3, pp. 92-96, Sept. 2008.

[4] RFID Journal, “Italian Textile Firms Rolls Over to RFID,” The History of RFID Technology - 2005-01-16 - Page 1 - RFID Journal. [Online]. Available: https://www.rfidjournal.com/articles/view?3515. [Accessed: 05-Mar-2019].

[5] A. Kiourti, “RFID Antennas for Body Area Applications: from Wearables to Implants,” IEEE Antennas and Propagation Magazine, vol. 60, no. 5, pp. 14-25, Aug. 2018.

[6] S. Shao, A. Kiourti, R. J. Burkholder, and J. L. Volakis, “Broadband Textile-Based Passive UHF RFID Tag Antenna for Elastic Material,” IEEE Antennas and Wireless Propagation Letters, vol. 14, pp. 1385–1388, 2015.

[7] R. Colella and L. Catarinucci, “Wearable UHF RFID Sensor Tag in 3D-Printing Technology for Body Temperature Monitoring,” 2018 2nd URSI Atlantic Radio Science Meeting (AT-RASC), 2018.

[8] “RFID Range,” SkyRFID Inc. [Online]. Available: https://skyrfid.com/RFID_Range.php. [Accessed: 19-Mar-2019].

[9] Aguirre, Juan I. Epcglobal: A Universal Standard. , 2007. Print.

[10] “NORDIC ID STIX,” Nordic ID Group. [Online]. Available: https://www.nordicid.com/device/nordic-id-stix/. [Accessed: 05-Mar-2019].

[11] “Confidex,” Confidex :: Smart Mobility. [Online]. Available: https://www.confidex.com/. [Accessed: 05-Mar-2019].

[12] S. Smiley, “RF Physics: How Does Energy Flow in an RFID System?,” RFID Insider, 30-Mar-2018. [Online]. Available: https://blog.atlasrfidstore.com/rf-physics. [Accessed: 05-Mar-2019].

[13] “EM Microelectronic,” Tailor-Made chips and modules manufacturer. [Online]. Available: https://www.emmicroelectronic.com/. [Accessed: 05-Mar-2019].

[14] “ANSYS,” Engineering Simulation & 3D Design Software. [Online]. Available: https://www.ansys.com/. [Accessed: 05-Mar-2019].

[15] G. Marrocco, “The art of UHF RFID antenna design: impedance-matching and size-reduction techniques,” IEEE Antennas and Propagation Magazine, vol. 50, no. 1, pp. 66–79, 2008.

[16] S. Uda and Y. Mushiake, Yagi-Uda Antenna, Tokyo, Sasaki Printing and Publishing Co., 1954, pp. 119-131.

[17] C. A. Balanis, Antenna theory: analysis and design. Hoboken (NJ): Wiley-Interscience, 2016.

[18] J. Zhong, A. Kiourti, T. Sebastian, Y. Bayram, and J. L. Volakis, “Conformal Load-Bearing Spiral Antenna on Conductive Textile Threads,” IEEE Antennas and Wireless Propagation Letters, vol. 16, pp. 230–233, 2017.

[19] P. V. Nikitin, K. V. S. Rao, S. F. Lam, V. Pillai, R. Martinez, and H. Heinrich, “Power reflection coefficient analysis for complex impedances in RFID tag design,” IEEE Transactions on Microwave Theory and Techniques, vol. 53, no. 9, pp. 2721–2725, 2005.

[20] A. Kiourti, C. Lee, and J. L. Volakis, “Fabrication of Textile Antennas and Circuits With 0.1 mm Precision,” IEEE Antennas and Wireless Propagation Letters, vol. 15, pp. 151–153, 2016.

[21] R. Vilkhu, W. J.-C. Thio, P. D. Ghatak, C. K. Sen, A. C. Co, and A. Kiourti, “Power Generation for Wearable Electronics: Designing Electrochemical Storage on Fabrics,” IEEE Access, vol. 6, pp. 28945–28950, 2018.

Appendix A: Acronyms and Abbreviations

RFID	Radio Frequency Identification
RF	Radio Frequency
NFC	Near Field Communication
LF	Low Frequency
HF	High Frequency
UHF	Ultra-High Frequency
EM	Electromagnetic
BAP	Battery-Assisted Passive
ISO	International Organization for Standardization
IC	Integrated Circuit
HFSS	High Frequency Structure Simulator
PCB	Printed Circuit Board
PEC	Perfect Electric Conductor
VNA	Vector Network Analyzer
SMA	Subminiature Version A
RSSI	Received Signal Strength Indication